# Melanocytes in black-boned chicken have immune contribution under infectious bursal disease virus infection

Deping Han,[*,1] Yurong Tai,[†,1] Guoying Hua,[†] Xue Yang,[†] Jianfei Chen,[†] Junying Li,[†] and Xuemei Deng[†,2]

[*]*College of Veterinary Medicine, China Agricultural University, Beijing 100193, China; and* [†]*Key Laboratory of Animal Genetics, Breeding and Reproduction of the Ministry of Agriculture & Beijing Key Laboratory of Animal Genetic Improvement, China Agricultural University, Beijing 100193, China*

**ABSTRACT** In black-boned chicken, melanocytes are widely distributed in their inner organs. However, the roles of these cells are not fully elucidated. In this study, we used 3-wk-old female Silky Fowl to investigate the functions of melanocytes under infection with infectious bursal disease virus (**IBDV**). We found the melanocytes in the bursa of Fabricius involved in IBDV infection shown as abundant melanin were transported into the nodule and lamina propria where obvious apoptotic cells and higher expression of BAX were detected. Genes related to the toll-like receptor (**TLR**) signaling pathway were highly detected by quantitative PCR, including *TLR1, TLR3, TLR4, TLR15*, myeloid differential protein-88, interferon-$\alpha$, and interferon-$\beta$. We then isolated and infected primary melanocytes with IBDV in vitro and found that higher expressions of immune genes were detected at 24 and 48 h after infection; the upregulated innate and adaptive immune genes were involved in the pathogenesis of IBDV infection, including *TLR3, TLR7*, interleukin 15 (*IL15*), *IL18, IL1rap, CD7, BG2, ERAP1*, and *SLA2*. These changes in gene expression were highly associated with microtubule-based movement, antigen processing and presentation, defense against viruses, and innate immune responses. Our results indicated that the widely distributed melanocytes in Silky Fowl could migrate to play important innate immune roles during virus infection.

**Key words:** melanocyte, avian, mucosal immunity, infectious bursa disease virus

2021 Poultry Science 100:101498
https://doi.org/10.1016/j.psj.2021.101498

## INTRODUCTION

In most vertebrates, melanocytes mainly exist in the epidermis and hair bulb, which produce eumelanin and phaeomelanin to protect the skin from sunburn (Chang et al., 2017) and allow for the generation of diverse skin, hair, and feather colors (Morgan et al., 2018; Anello et al., 2019; Domyan et al., 2019; Henkel et al., 2019; Hofstetter et al., 2019). In black-boned chicken, the melanocytes are not confined in the epidermis, and also widely located in the dermis and inner organs (Dorshorst et al., 2010). In most vertebrates, melanocytes only exhibit dorsal migration at the embryo stage, but melanocytes in black-boned chicken also programmed ventral migration, resulting in a wide distribution of melanocytes in the inner organs such as thymus, bursa of Fabricius (**BFs**), testis, ovary, brain, lungs, and kidneys (Faraco et al., 2001; Dorshorst et al., 2011; Shinomiya et al., 2012; Han et al., 2015). As for the Silky Fowl (**SF**), the melanocytes are widely observed in their inner organs and skin but which are not found in the epidermis and only locate around hair follicles in the dermis, yielding their white feathers (Han et al., 2015). In these inner organs, melanocytes with long dendrites surround the blood vessels and have close relationships with neighboring cells (Han et al., 2015; Han et al., 2017). However, besides producing melanin giving hyperpigmentation phenotype, the roles of the widely distributed melanocytes in SF are still veiled.

Previous study has found that the melanocytes in zebra fish could engulf exogenous bead and then recruit immune cells to protect from injury (Levesque et al., 2013). Wang and coworkers found the macrophage-like melanocytes in the inner ear could anchor on the blood vessels to maintain the permeability prohibiting hearing loss (Zhang et al., 2012). On account of the previously reported roles of melanocytes in other vertebrates, what are the roles of widely distributed melanocytes in the SF

© 2021 The Authors. Published by Elsevier Inc. on behalf of Poultry Science Association Inc. This is an open access article under the CC BY-NC-ND license (http://creativecommons.org/licenses/by-nc-nd/4.0/).

Received March 1, 2021.
Accepted September 16, 2021.

[1]These authors contributed equally to the work.

[2]Corresponding author: deng@cau.edu.cn

needs to be elucidated. In our previous studies, we found that the migration of atypical melanocytes during embryo stage could result in aberrant immune system development in SF (Han et al., 2015; Han et al., 2017) when we conclude the weak immune development at early stages is beneficial for melanocyte migration into inner organs. In human, the melanocytes could transform into melanoma cells which could inhibit immune responses to achieve their metastasis (Byrne and Fisher, 2017; Natale et al., 2018). But as for SF, the wide distribution of melanocytes is not a pathological feature; thus, elucidation of melanocyte function could improve our understanding of the mechanisms of melanoma morphogenesis.

## MATERIALS AND METHODS

### Virus

A virulent strain of Infectious bursal disease virus (**IBDV**; BC6/85, CVCC AV7) was obtained from China Institute of Veterinary Drug Control (Beijing, China) (Ma et al., 2013; Zhao et al., 2016). The pathogenicity indices were $10^3$ 50% egg infective doses (**EID50s**), and the virus stock was prepared by growing the virus in 10-day-old SPF embryonating chicken eggs and was subsequently stored at −80°C until further use.

### Birds and Treatment

Twenty-four female SFs (3 wk of age) were obtained from the animal farm of China Agricultural University, Beijing and divided into the control (n = 12) and infection groups (n = 12). SFs in the infection group were inoculated with $10^3$ 50% EID50s IBDV in 0.1 mL by eye drops, and SFs in the control group were inoculated with 0.01 M phosphate-buffered saline. The chickens were sacrificed by severing the jugular veins after anesthesia, bled for 3 to 5 min, and then dissected. The BFs were sampled at 1, 3, 5, and 7 d postinfection (**dpi**), and were cut into 2 along the sagittal plane; one half was fixed in 4% paraformaldehyde solution (Beijing Solarbio Life Science and Technology Co., LTD, Beijing, China), and the other half was stored in liquid nitrogen.

The protocols for animal use and experimentation were approved by the Beijing Association for Science and Technology (approval ID SYXK [Beijing] 2007 −0023) and were in compliance with the Beijing Laboratory Animal Welfare and Ethics guidelines. All animal research work was also approved by the Beijing Administration Committee of Laboratory Animals, and was in accordance with the China Agricultural University (CAU) Institutional Animal Care and Use Committee guidelines (ID: SKLAB-B-2010−003).

### Histological Observation

After fixation in 4% paraformaldehyde solution for a minimum period of 24 h before use, the BFs were trimmed, dehydrated by alcohols, and embedded in paraffin. After that, 5 $\mu$m serial sections were made. The sections were dewaxed, rehydrated, and incubated in Hematoxylin solution (Zhongshan GoldenBridge Biotechnology Co. LTD, Beijing, China) for 10 min. After being rinsed with distilled water, the sections were rinsed with 1% hydrochloric acid in 75% alcohol for 10 s, and then incubated in phosphate-buffered saline (pH 7.2) for 15 min. The sections were incubated in 70% and 80% alcohol for 3 min respectively, and then were stained with Eosin solution (Zhongshan GoldenBridge Biotechnology Co. LTD, Beijing, China) for 20 s. After destained in 95% alcohol for 1 min, the sections were dehydrated in 100% alcohol and xylene for 5 min, and then were mounted with neutral balsam for observation under light microscope. The histopathological changes were observed and pictured using a Zeiss camera system (Carl Zeiss Optics Co. LTD, Guangzhou, China).

### Immunofluorescence

The fixed BFs were trimmed and dehydrated by 30% and 50% sucrose solution, and then embedded in OCT (Opti-mum Cutting Temperature compound, Leica, Shanghai, China) to prepare 5 $\mu$m frozen sections. Sections were washed with distilled water and then incubated in 3% hydrogen peroxide solution (Beijing Solarbio Life Science and Technology Co., LTD, Beijing, China) for 15 min at room temperature. After washed with the distilled water, the sections were blocked with 1% bovine serum albumin (Beijing Solarbio Life Science and Technology Co., LTD, Beijing, China) for 20 min at room temperature. The sections were incubated with primary monoclonal antibody rabbit anti-Bax (Santa Cruz, TX, 1:200) overnight at 4°C. After rinsed with PBS, sections were reacted with goat antirabbit IgG conjugated with fluorescein isothiocyanate (Zymed Laboratories Inc, Beijing, China) at room temperature for 1 h. After rinsing with PBS, the sections were observed and pictured using Zeiss camera system (Carl Zeiss Optics Co. LTD, Guangzhou, China). In the negative control, the primary antibody was replaced with PBS.

### Immunohistochemistry

Frozen sections were washed with distilled water, incubated in 3% hydrogen peroxide solution for 15 min at room temperature, washed with distilled water again, and blocked with 1% bovine serum albumin for 20 min at room temperature. The sections were incubated with primary mouse monoclonal antibody against viral protein 2 (**VP2**) (a gift from Harbin Veterinary Research Institute, Chinese Academy of Agricultural Sciences, Harbin, China; 1:1000) overnight at 4°C. After rinsing with PBS, the sections were treated with goat antimouse immunoglobulin G (**IgG**) conjugated to horseradish peroxidase (Zhongshan Golden Bridge Biotechnology, Beijing, China) at room temperature for 1 h. After treating the sections with chromogen diaminobenzidine (Zhongshan

Golden Bridge Biotechnology, Beijing, China) for 10 min at room temperature in the dark, the sections were counterstained with hematoxylin. The primary antibodies were replaced with PBS in the negative controls.

## TUNEL Staining

The presence of apoptotic cells was determined using the In Situ Cell Death Detection Kit (Roche, Philadelphia, PA). Paraffin-embedded sections of BFs were dewaxed, rehydrated according to standard procedures, and immersed in a plastic jar containing 200 mL of citrate buffer (0.1 M, pH 6.0). The slides were subjected to microwave irradiation (750 W [high]) for 1 min, cooled rapidly by immediately adding 80 mL of double-distilled water, and then transferred into PBS. The slides were immersed for 30 min in Tris-HCl (0.1 M, pH 7.5, containing 3% BSA and 20% normal bovine serum) and then rinsed twice with PBS. The preceding steps were performed at 20°C to 25°C. The TUNEL reaction mixture was added to the slides, which were then incubated at 37°C in a humidified atmosphere in the dark for 60 min. The slides were rinsed 3 times in PBS for 5 min each. Samples were analyzed in a drop of PBS using a fluorescence microscope with excitation and detection wavelengths of 450 to 500 nm and 515 to 565 nm (green), respectively. The TUNEL reaction mixture was replaced with label solution in the negative control.

## Primary Melanocytes and IBDV Infection

The primary melanocytes used in this work are isolated and cultured as previous reported (Han et al., 2015), the SF fertilized eggs hatched at 15 d were collected from the farm in China Agricultural University, and the peritoneum was sampled to dissociate primary melanocytes. The peritoneum was dissected and washed in PBS for 3 times at room temperature. Specimens were cut into pieces in Medium 254 (Thermo Fisher Scientific Inc., Shanghai, China), and then digested for 15 min in 0.1 mg/mL Dispase 2 (Roche, Philadelphia, PA) and Trypsin-ethylenediamine teacetic acid solution (Thermo Fisher Scientific Inc., Shanghai, China). After termination with fetal bovine serum (Thermo Fisher Scientific Inc., Shanghai, China), we filtered the digests through a cell strainer and then centrifuged them for 10 min at 1000 r/min. The cell pellets were resuspended with modified Medium 254 (10 mL Human Melanocyte Growth Supplement [Thermo Fisher Scientific Inc., Shanghai, China] in 500 mL medium). According to the good adhesion, the melanocytes were purified according to the various digestions (3, 5, and 10 min) and adherence times (0.5, 1, and 2 h) during their passages in culture. The specificities of melanocytes were further confirmed by morphology, ultrastructure observation under electron transmission microscope, genes expression associated with melanin synthesis, and cell characteristic by dihydroxyphenylalanine stain and transcription factors associated with microphthalmia immunocytochemistry. The melanocytes with a single layer were inoculated with $10^3$ 50% EID50s IBDV in 0.5 mL for 2 h at 37°C 5% $CO_2$ incubator. After discarding the virus, the melanocytes were rinsed with PBS for 2 times, and then were added with fresh Medium 54 for culture. At 24 h and 48 h postinfection (hpi), the melanocytes in 6 well plate with 3 duplications were collected and detected for RNA sequencing.

## RNA Sequencing and Data Analysis

Total RNA was isolated from melanocytes using the Invitrogen TRIzol reagent (Thermo Fisher Scientific Inc., Beijing, China) according to the manufacturer's instructions. We visualized RNA degradation and contamination on 1% agarose gels; RNA purity was checked using a NanoPhotometer spectrophotometer (IMPLEN), and concentrations were determined using the Qubit RNA Assay Kit in Qubit 2.0 Fluorometer (Life Technologies, Shanghai, China). We assessed RNA integrity using the RNA Nano 6000 Assay Kit of the Bioanalyzer 2100 system (Agilent Technologies, Beijing, China), and a total of 3 $\mu$g of RNA from each sample was used as the input material for RNA sample preparations. The ribosomal RNA was removed using an Epicentre Ribo-zero rRNA Removal Kit (Epicentre), and the mRNA sequencing libraries were constructed using an NEBNext Ultra Directional RNA Library Prep Kit for Illumina (NEB), according to the manufacturer's recommendations. We then sequenced the mRNA libraries on an Illumina Hiseq 2000 platform and generated 100-bp paired-end reads.

The transcriptome sequencing and analysis were conducted by OE biotech Co., Ltd. (Shanghai, China). Raw data (raw reads) were processed using Trimmomatic. The reads containing poly-N and the low-quality reads were removed to obtain the clean reads. Then, the clean reads were mapped to Gallus gallus genome website (ftp://ftp.ensembl.org/pub/release-74/fasta/gallus_gallus/dna/) using hisat2 (Kim et al., 2013). FPKM value of each gene was calculated using cufflinks, and the read counts of each gene were obtained by htseq-count. FPKM and the read counts value of each transcript (protein coding) were calculated using Bowtie2 and eXpress. DEGs were identified using the DESeq. R package functions estimate SizeFactors and nbinomTest. $P$ value $< 0.05$ and foldChange $>2$ or foldChange $<0.5$ was set as the threshold for significantly differential expression. Hierarchical cluster analysis of DEGs was performed to explore genes expression pattern. GO enrichment of differentially expressed genes (**DEGs**) was respectively performed using R based on the hypergeometric distribution.

## RNA Extraction and Quantitative Real-Time PCR (qPCR)

Total RNA from frozen FBs samples were extracted by using Invitrogen TRIzol reagent (Thermo Fisher Scientific Inc., Shanghai, China) following the manufacturer's instructions. RNA degradation and contamination were visualized on 1% agarose gels. RNA purity was checked

using a NanoPhotometer spectrophotometer (IMPLEN, Beijing, China), and concentrations were determined using the Qubit® RNA Assay Kit in Qubit® 2.0 Fluorometer (Life Technologies, Shanghai, China). A total of 1 $\mu$g RNA was reverse transcribed into cDNA using the Fast Quant RT Kit (with gDNase) (Tiangen Biotech Co. LTD, Beijing, China) according to manufacturer's instructions. The expression levels of the toll-like receptor 1 (***TLR1***), *TLR2, TLR3, TLR4, TLR5, TLR7, TLR15, TLR21*, myeloid differential protein-88 (*MyD88*), tumor necrosis factor receptor-associated factors-3 (*TRAF3*), *TRAF6*, interferon-$\alpha$ (*IFN$\alpha$*), *IFN$\beta$*, and IBDV-VP2 were quantified with qPCR using the SYBR Green Real-time PCR Master Mix (Tiangen Biotech Co. LTD, Beijing, China). The primers for qPCR were designed using the Primer Premier 5 software (PREMIER Biosoft, Palo Alto, CA) and were subsequently synthesized (Sangon Biotech Co. LTD, Beijing, China). The primer information is listed in Table 1. The cycling parameters used for qPCR amplification were as follows: initial heat-denaturation at 95°C for 4 min; 40 cycles of 95°C for 30 s, 55 to 60°C for 30 s, and 72°C for 30 s; and a final extension at 72°C for 5 min. A melting curve analysis was performed to exclude genomic DNA contamination and to confirm primer specificities. Gene expression was normalized using the $2^{-\triangle\triangle CT}$ method with the glyceraldehyde 3-phosphate dehydrogenase (*GAPDH*) gene as an internal standard. Each biological duplicate was controlled in 3 technical replicates.

### Statistical Analysis

All statistical analyses were performed using Prism 6.0 (GraphPad Software, San Diego, CA). Data are expressed as means ± standard error of the mean (SEM). Statistical significance was evaluated using Student's $t$ test. Asterisk coding is indicated in the Figure Legends as $^{*}P < 0.05$; $^{**}P < 0.01$.

## RESULTS

### Melanocytes Involved in IBDV Infection

By histology, we observed in the BFs that melanocytes with long dendrites widely distributed between the bursal nodules (Figures 1A and 2A). On d 1 after IBDV infection, no obvious pathological changes were observed for the morphology of melanocyte, but severe cell death was induced at 3, 5, and 7 dpi (Figure 1). The melanocytes formed a large number of apoptotic bodies (Figures 1 and Figures 2C and 2D), accompanied by ubiquitous scattering of melanin in the bursal nodules and lamina propria (Figures 1 and 2B). Beside melanocytes, B cell apoptosis was significantly induced at 5 and 7 dpi (Figures 3A and 3B) accompanied with obvious hemorrhage and atrophy of bursal nodules (Figures 1C and 1D), and the proapoptotic protein BAX was highly expressed in the epithelial cells, melanocytes, and B cells of IBDV-infected BFs from 1 dpi to 7 dpi (Additional file 2).

### Higher Expressions of Innate Immune Genes in the BFs

To detect the immune responses of BFs of SF after infection with IBDV, we firstly detected the expression levels of IBDV VP2. It is found the virus could replicate in the BFs of SF (Figures 3C and 3D) which was significantly

**Table 1.** The primers used to detect the targeted genes by qPCR.

| Genes | Primer sequence (5'-3') | Annealing temperature | Accession number |
|---|---|---|---|
| *TLR1* | F-GCTGTGTCAGCATGAGAGGA<br>R-GTGGTACCTCGCAGGGATAA | 59°C | NM_001007488.4 |
| *TLR2* | F-GAA AGTTCCCCCTTTTCCAG<br>R-AGAGTGCAGAAGGTCCCTGA | 56°C | NM_001161650.2 |
| *TLR3* | F-CCGCCTAAATATCACGGTAC<br>R-GCGTCATAATCAAACACTCCC | 60°C | NM_001011691.3 |
| *TLR4* | F-GCTGGGCAAAGTGAAAAGAG<br>R-TAAGAACAGCCCGTTCATCC | 57°C | NM_001030693.1 |
| *TLR5* | F-TCACACGGCAATAGTAGCAAC<br>R-CCTGAACACATCCAAACATAA | 57°C | NM_001024586.1 |
| *TLR7* | F-CCTGACCCTGACTATTAACCAT<br>R-CGTAAAGTAGCAGGAAGACCC | 57°C | NM_001011688.2 |
| *TLR15* | F-AACATCTACATCCGTAACCCG<br>R-TTAGCACCAGAACGACAAGG | 56°C | NM_001037835.1 |
| *TLR21* | F-CAAGAAGCAGCGGGAGAAG<br>R-TCAGGATGCGGTTAAAGCG | 57°C | NM_001030558.2 |
| *IBDV-VP2* | F-AGAGCTGTGGCCGCAGACAAT<br>R-TGGATAGTTGCCACCGTGGAT | 60°C | MN464103.1 |
| *MyD88* | F-ACCTGGAAAGTGATGAATGT<br>R-TTGTAATGAACCGCAAGATA | 56°C | NM_001030962.4 |
| *TRAF3* | F-GGGACGCACTTGTCGCTGT<br>R-ACTGCTGCTGTTTGGATCTGG | 60°C | XM_025150935.2 |
| *TRAF6* | F-ATGGAAGCCAAGCCAGAGTT<br>R-ACAGCGCACCAGAAGGGTAT | 56°C | XM_004941548.4 |
| *IFN-α* | F-CAGGATGCCACCTTCTCTCAC<br>R-AGGATGGTGTCGTTGAAGGAG | 60°C | NM_205427.1 |
| *IFN-β* | F-CCTCAACCAGATCCAGCATTAC<br>R-CCCAGGTACAAGCACTGTAGTT | 58°C | NM_001024836.1 |
| *GAPDH* | F- AAAGTCCAAGTGGTGGCCATC<br>R-TTTCCCGTTCTCAGCCTTGAC | 55–60°C | NM_204305.1 |

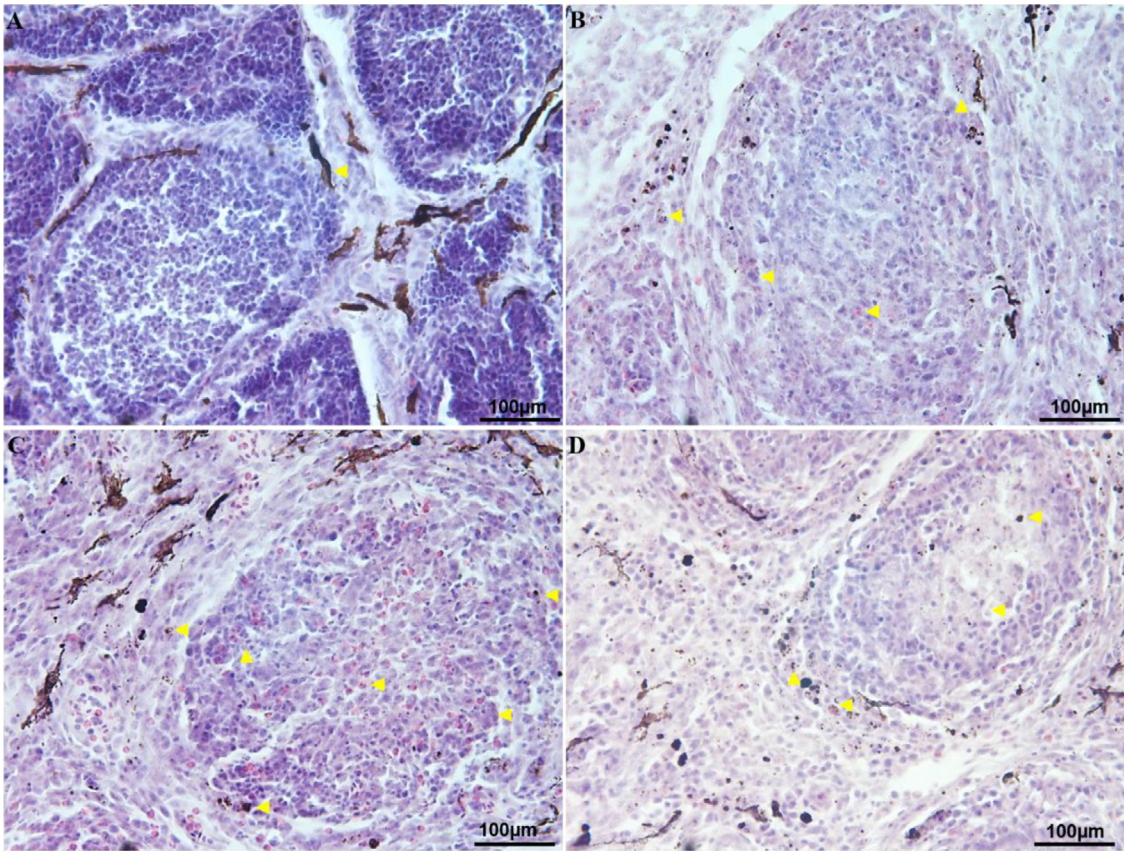


**Figure 1.** Melanocytes showed obvious apoptosis in the BFs after IBDV infection. (A) On 1 dpi, no obvious pathological changes were observed in the BFs when melanocytes with long dendrites were observed. (B) Melanin was scattered in the nodule and lamina propria, and few red blood cells infiltrated in the nodule on 3 dpi. (C) More melanin and red blood cells infiltrated the nodule and lamina propria, and obvious B-cell apoptosis was observed on 5 dpi. (D) On 7 dpi, abundant melanin infiltrated in the nodule and lamina propria, and fewer B cells were in the medulla of the nodule.

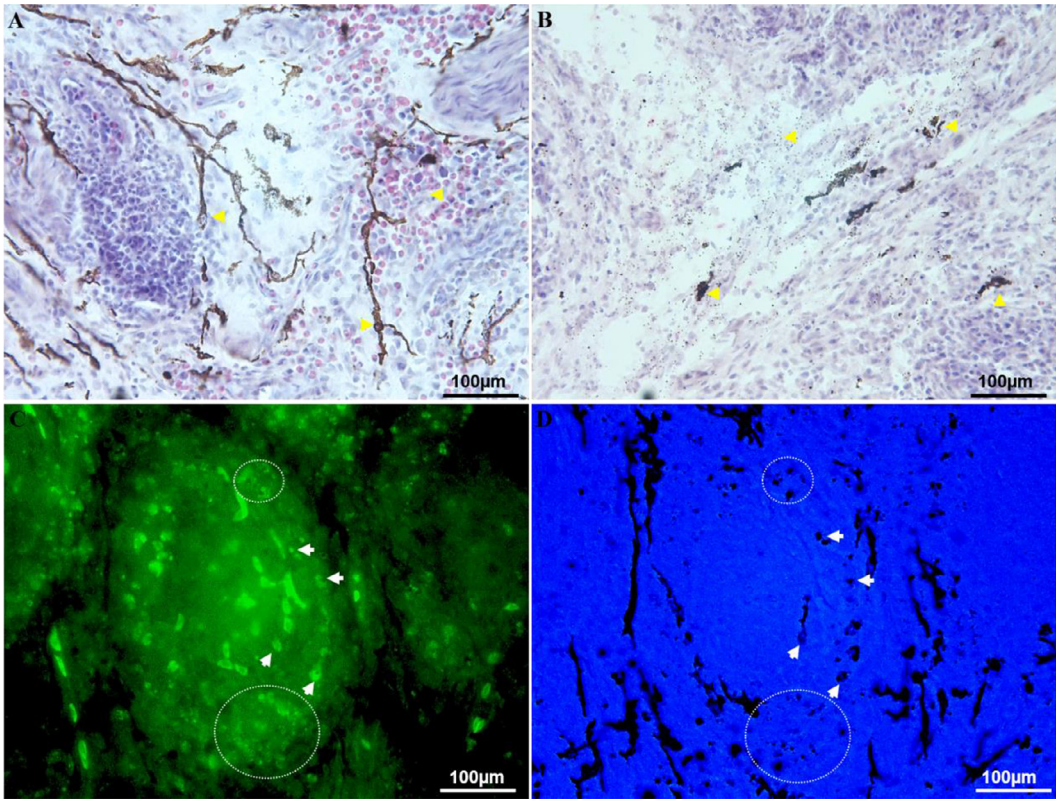


**Figure 2.** Higher expression of BAX protein was closely related to the melanocyte and B cell apoptosis. (A) Melanocytes with long dendrites and heterophilic granulocytes were observed in the control BFs. (B) Severe disruption of melanocytes with lots of melanin was scattered in the IBDV-infected BFs on 7 dpi. (C) BAX proteins were detected in the in the nodule and lamina propria after immunofluorescence staining. (D) Under the white field of vision, obvious apoptosis of melanocytes was observed (arrow and dotted circle).

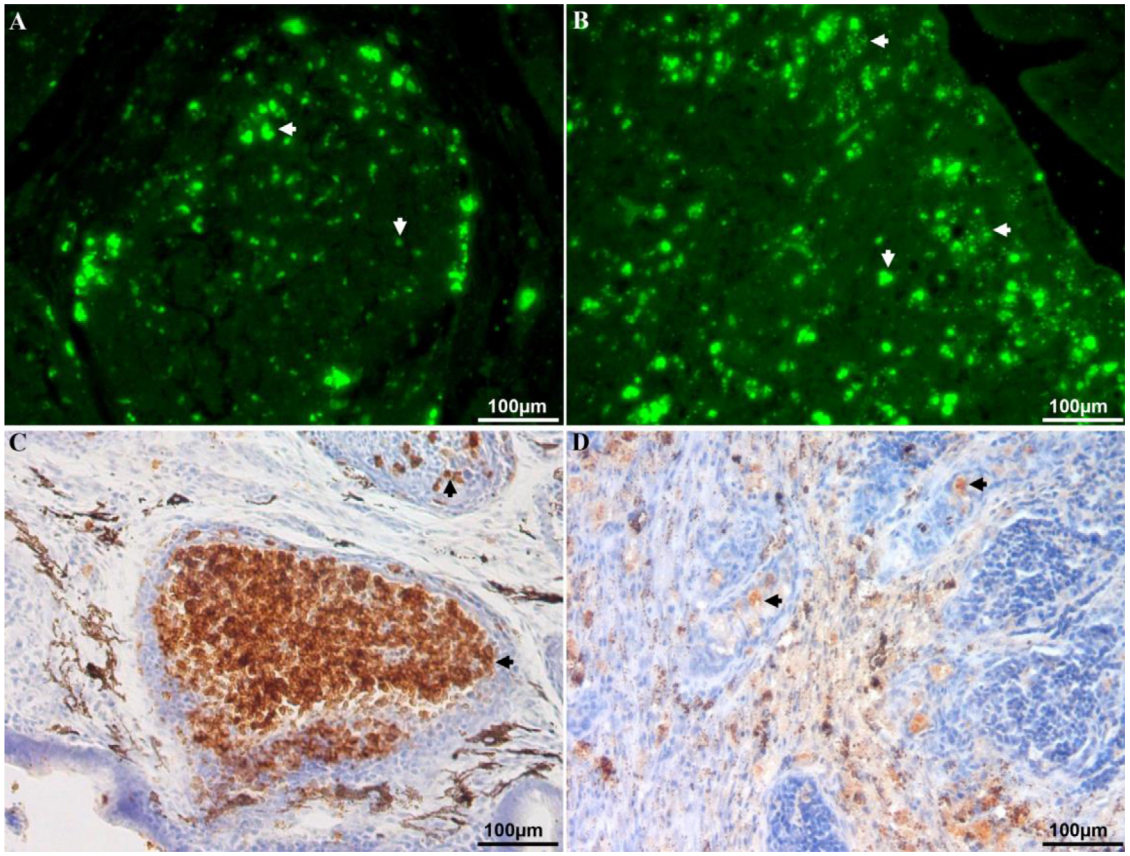


**Figure 3.** Obvious apoptosis and virus replication were in the BFs after IBDV infection. (A) Apoptotic cells were significantly detected in the bursal nodules at 5 dpi by TUNEL staining. (B) Severe apoptosis with obvious apoptotic bodies was induced in the lamina propria and bursal nodules on d 7 after IBDV infection. (C) Higher expression of IBDV VP2 proteins was detected in some capsules of BF at 5 dpi. (D) Lots of melanin but fewer IBDV VP2 proteins were in the BF on d 7.

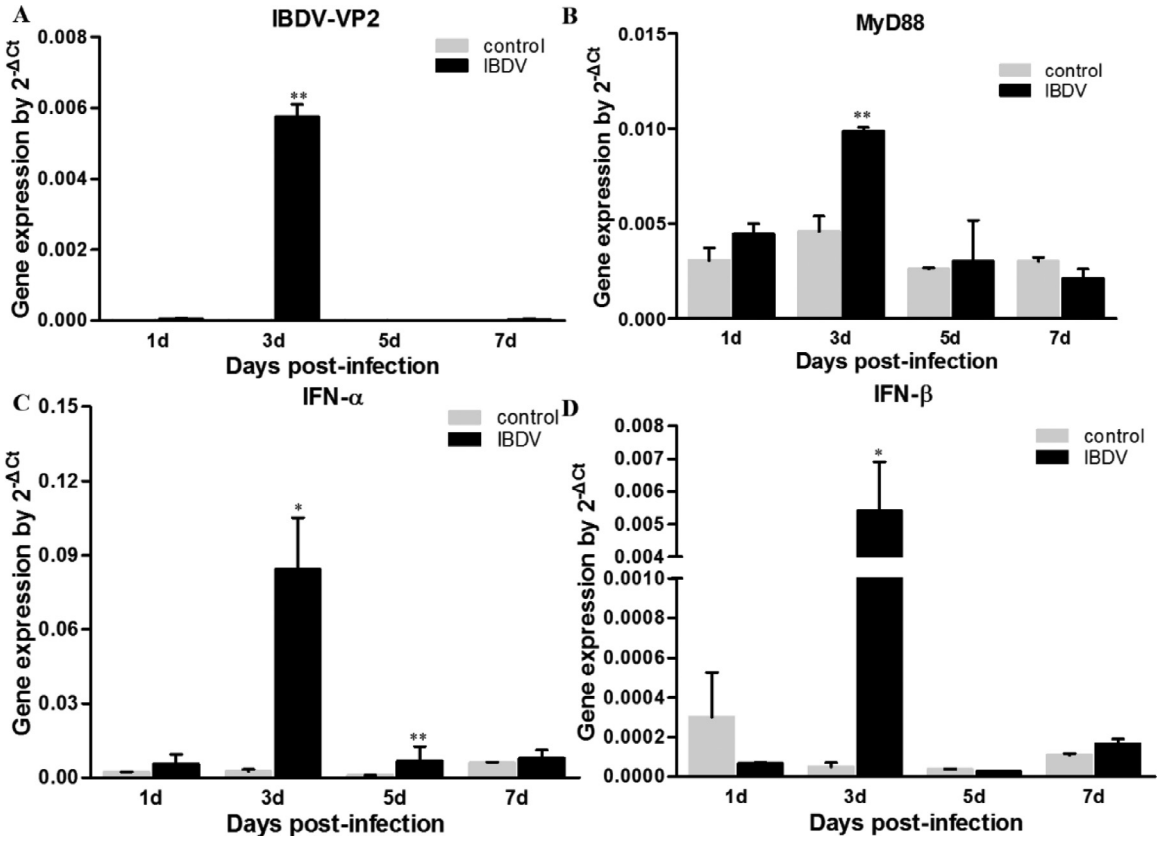


**Figure 4.** Expression of genes related to the TLR signaling pathway. The genes of (A) *TLR1*, (B) *TLR3*, (C) *TLR4*, and (D) *TLR15* were highly detected in the BFs on d 3 and 5 after IBDV infection ($^*P < 0.05$, $^{**}P < 0.01$).

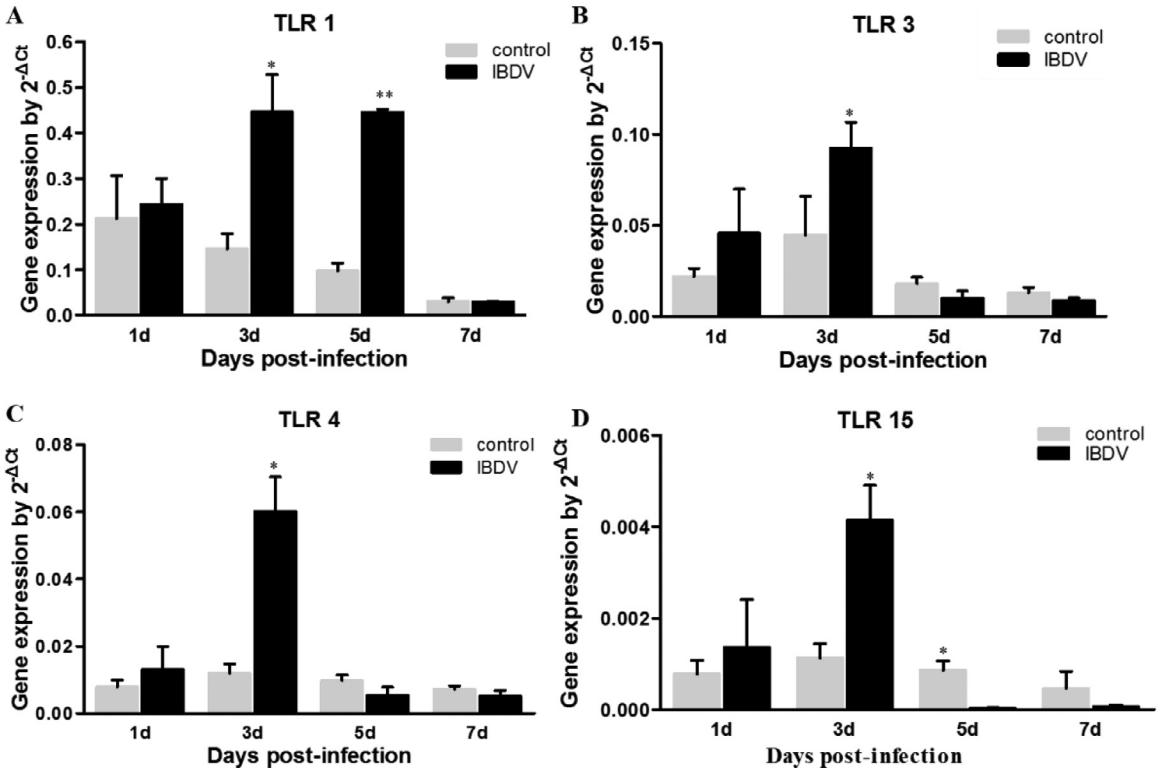


**Figure 5.** Expression of genes related to immune response in the BFs. (A) Obvious virus replication was detected on d 3 after infection. The genes of (B) *MyD88*, (C) *IFN-α*, and (D) *IFN-β* were highly detected on d 3 and 5 after IBDV infection (*$P < 0.05$, **$P < 0.01$).

detected at 3 and 5 dpi (Figures 3C and 3D, and 4A). By detecting the immune related genes, the antiviral cytokines interferon-$\alpha$ (*IFN-α*) and *IFN-β* showed higher expression at 3 dpi and 5 dpi (Figures 4C and 4D). And the genes associated with the toll-like receptor (TLR) signaling pathway were significantly up regulated including *TLR1, TLR3, TLR4, TLR15*, and *MyD88* (Figures 4B and 5), however, *TLR2, TLR7*, and *TRAF3* were down regulated (Additional file 3), and no significant changes in the *TLR5, TLR21*, and *TRAF3* (Additional file 3).

## Melanocytes Involved in the Immune Responses After IBDV Infection

In order to elucidate whether IBDV could infect melanocytes and to determine whether melanocytes expressed TLRs and which types of TLRs were associated with melanocyte responses, the primary melanocytes were isolated and exposed to IBDV. We observed that IBDV infection did not induce obvious cell death until 48 h post-infection (hpi), but the cell morphology was significantly changed, exhibiting dendrite elongation, cytoplasmic vesicle reduction, atrophy and lots of melanin were released (Figure 6). To ascertain whether the virus could infect melanocytes, we detected the expression of the IBDV *VP2* gene and found its expressions mildly increased at 24 ($P = 0.0366$) and 48 hpi ($P = 0.0265$; Figure 7A). We also detected the expression of *TLR3* and found its expression significantly increased at 24 ($P = 0.00034$) and 48 hpi ($P = 0.0097$; Figure 7B).

## Melanocytes Played Innate Immune Response During IBDV Replication

By analyzing the DEGs in the virus infected melanocytes, we tried to elucidate their immune response mechanism. The good differences within group and between groups is beneficial to analyze the DEGs (Additional file 4), and obvious differences of gene expressions were detected at 24 and 48 hpi (Additional file 5). By analysis, we found that innate and adaptive immune genes, such as *B2M, TLR3, TLR7, C1S, C1R, IL18, IL18BP, CXCL14*, and *LBP* significantly increased in the infected melanocytes (Figure 8), and the upregulated DEGs were highly enriched in antigen processing and presentation via MHC class I, MHC class I protein complex, microtubule-based movement, defense response to virus, innate immune response, and inflammatory response (Figure 9, additional file 1).

## Melanocytes Decreased Metabolism and Increased Motility and Phagocytosis

As shown in Figure 6, many vesicles were observed in control melanocytes; however, after IBDV infection, the vesicles were difficult to observe. Additionally, genes related to dopamine transport, lipid metabolic process, plasma membrane, and integral components of the plasma membrane were markedly decreased in the melanocytes. Thus, IBDV could

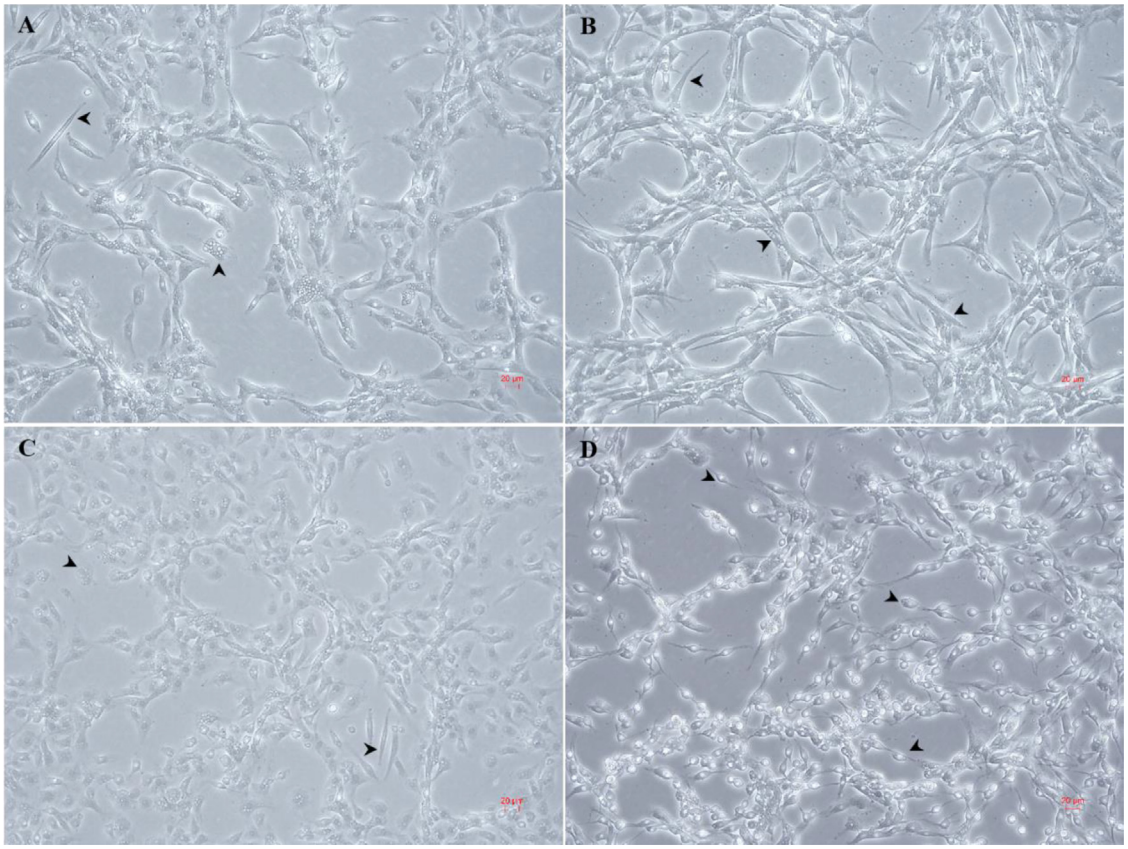


**Figure 6.** Melanocytes showed obvious pathological changes in vitro after IBDV infection. The melanocytes in the control group showed many vesicles in the cytoplasm, and obvious cell migration was observed at (A) 24 hpi and (C) 48 hpi. At (B) 24 h and (D) 48 h after IBDV infection, the melanocytes showed atrophy with reduced vesicle number and scattering of melanin in the extracellular space.

inhibit metabolic processes, vesicle formation, and transport. After IBDV infection, the melanocytes showed obvious elongation (Figure 6) and migration abilities (Additional file 1), and the specific surface molecule receptor genes *CD164, CD226, CD274, CD4*, and *CD7* were highly detected. At 48 hpi, genes associated with actin filament binding, actin cytoskeleton, positive regulation of actin filament polymerization, positive regulation of cell migration, and mesenchyme migration weakly expressed in the infected melanocytes (Additional file 1).

## DISCUSSION

IBDV is a causative agent of immunosuppressive disorder in the poultry which could induce severe pathological injury to the BFs. In poultry, the BFs provide the site for immature B lymphocytes to complete proliferation and differentiation, and as an important mucosal immune organ has key roles to identify pathogens and produce antibodies. At early development stage especially at 2 to 6 wk old, the immature development of BFs gives the chicken susceptibilities to IBDV infection

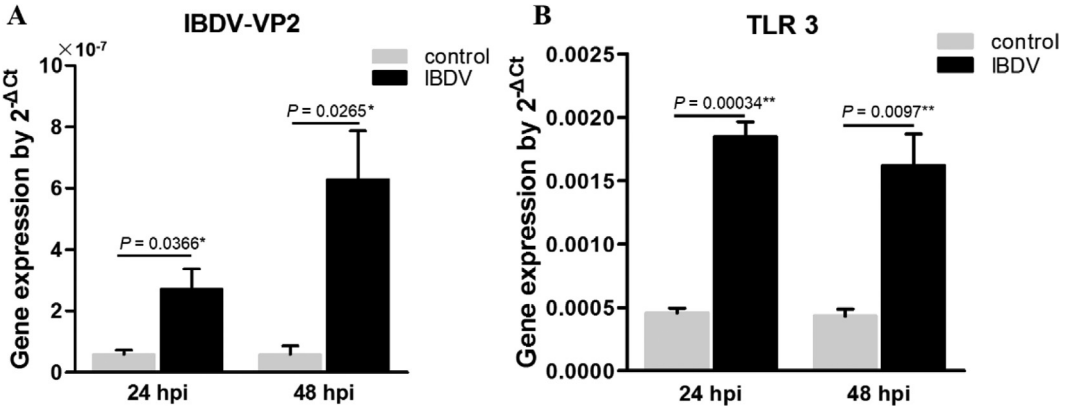


**Figure 7.** TLR3 and VP2 expression in the melanocytes after IBDV infection in vitro. Compared with control (A), The mRNA titers of IBDV VP2 in the melanocytes after IBDV infection in vitro. (B) Higher expressions of *TLR3* were detected in the melanocytes at 24 and 48 hpi.

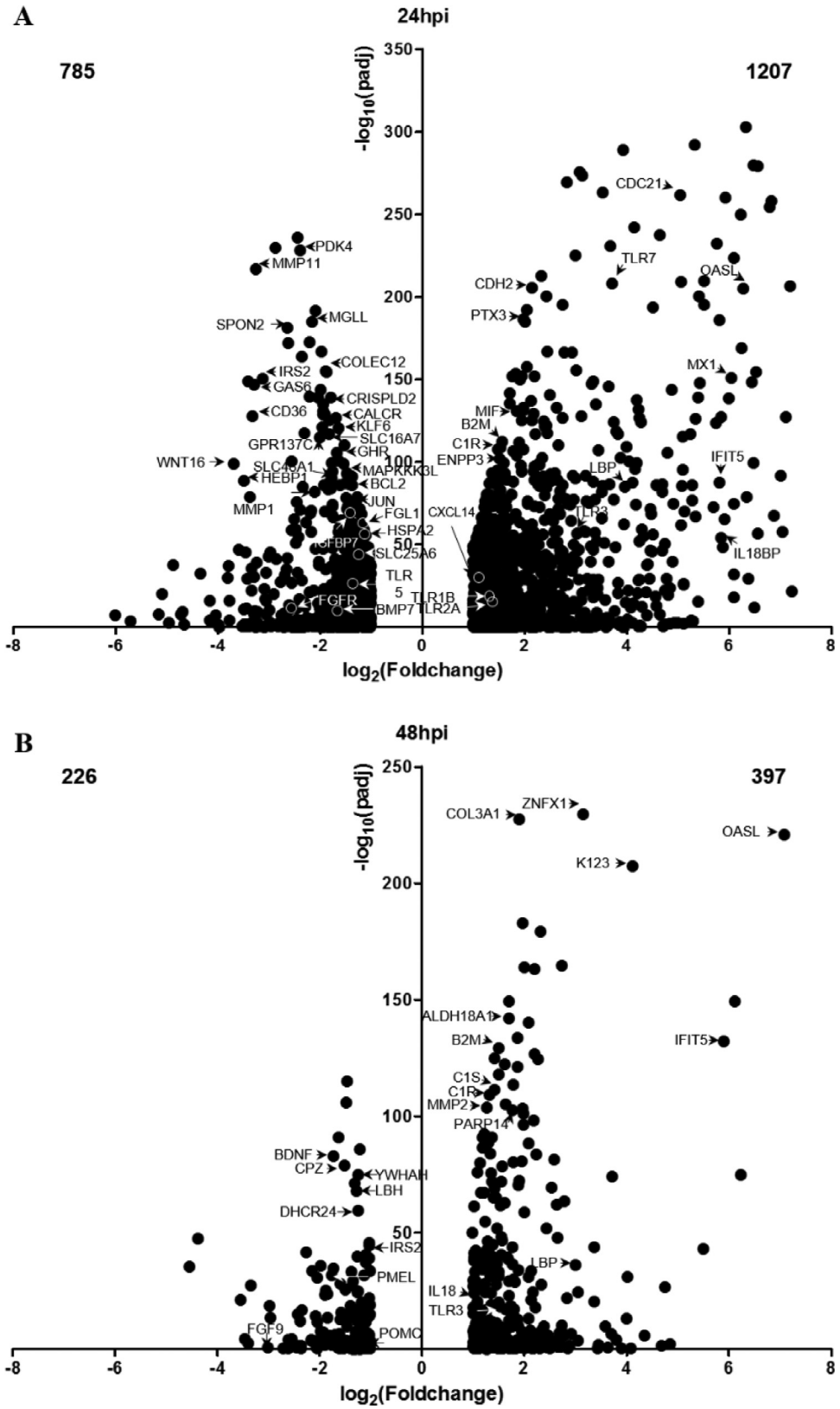


**Figure 8.** Differentially expressed genes in the melanocytes after IBDV infection. (A) At 24 hpi, 1,207 upregulated genes and 785 downregulated genes (Padjust < 0.05) were detected in the melanocytes, and the genes related to innate immune response were highly found in the upregulated genes. (B) Higher expression of innate immune genes and lower expression of melanin synthesized genes (Padjust < 0.05) were detected in the melanocytes.

(Muller et al., 2003; Yu et al., 2019; Lin et al., 2020). Additionally, beside development stage, it is noted that different chicken breeds show different susceptibilities to specific pathogens infection (Zekarias et al., 2000). Our previous study found the black-boned chicken SF have weak immune responses at the early development stage owing to the atypical melanocytes migration, which are widely present in almost all the inner organs, including

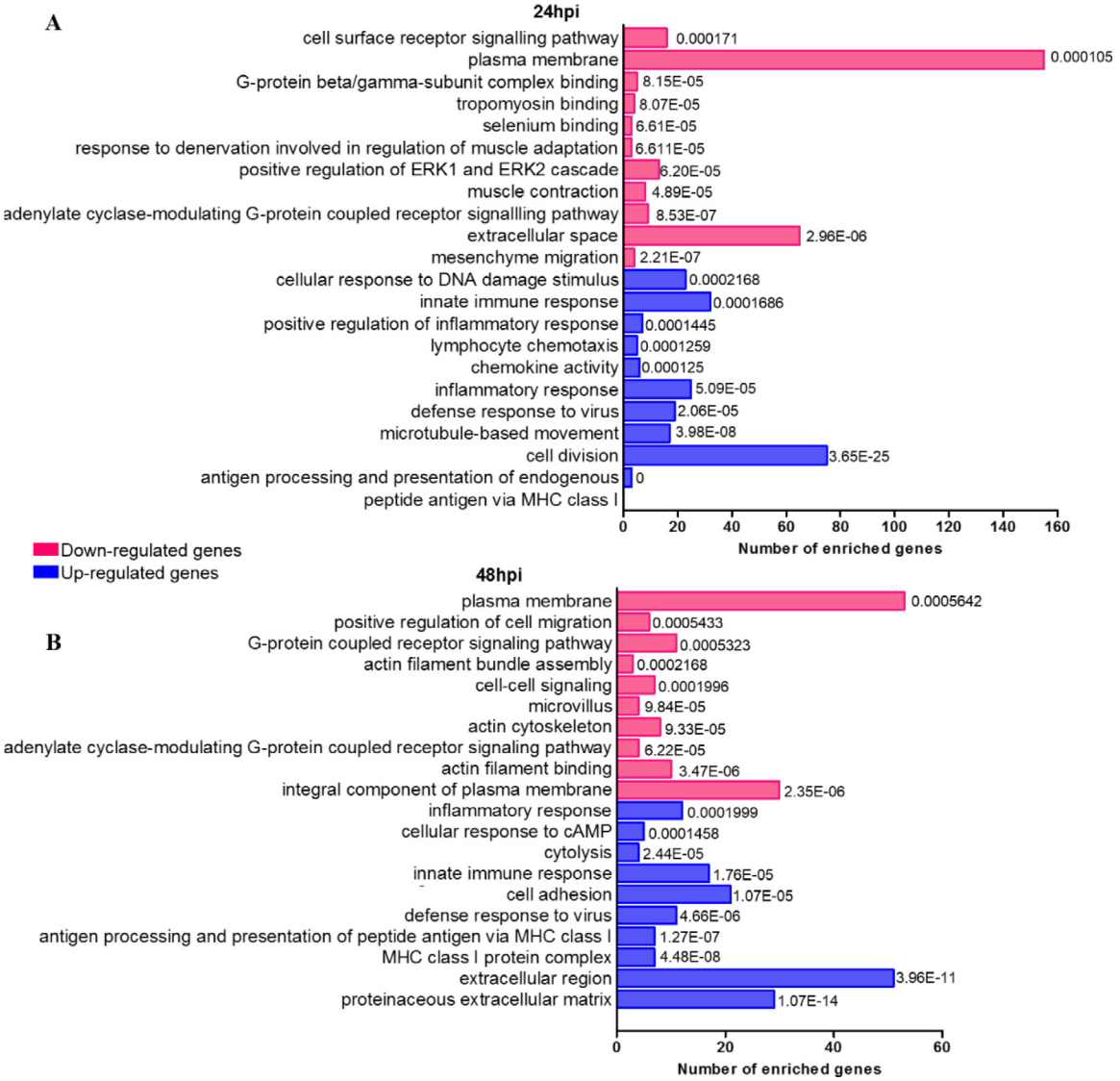


**Figure 9.** GO enrichment of differentially expressed genes in the melanocytes after IBDV infection. (A) At 24 hpi, the upregulated genes were highly enriched for antigen processing and presentation, lymphocyte chemotaxis, defense response to virus, and inflammatory response. (B) Innate immune response, MHC class protein complex, cytolysis, and extracellular region were highly enriched at 48 hpi.

the spleen, BFs, thymus, lung, and brain (Faraco et al., 2001; Ortolani-Machado et al., 2008; Han et al., 2015). During the clinical breeding of black-boned chicken, high mortality at the brood stage and infection rate of salmonella especially at the later laying period were concluded. Whether the widely distributed melanocytes were closely related to the pathogen infection is still veiled. In this work, we found IBDV could result in obvious apoptosis of melanocytes and induce higher expressions of TLR1, TLR3, TLR4, TLR15, MyD88, IFN-$\alpha$, and IFN-$\beta$ in the BFs. Additionally, it is found IBDV could infect and proliferate in the primary melanocytes from black-boned chicken and showed higher expression of genes associated with retinoic acid-inducible gene 1, endosomal TLR3 signaling pathway, and nucleotide-binding oligomerization domain-like receptor signaling pathway. So, the atypical migration and widely distribution of melanocytes in the BFs and other inner organs of the black-boned chicken at early development stages resulted in weak immune organs development giving them opportunities to some pathogen infection.

IBDV could infect the primary melanocytes, but very fewer IBDV were detected at 24 and 48 hpi and the VP2 protein were mainly detected in the B cells of BFs, which indicated the primary melanocytes were not the adequate sites for the IBDV infection and played immune roles for controlling IBDV infection. It has been found the melanocytes in human and other vertebrates have some contributions to antimicrobial infection, immune modulation, and barrier function, which is highly associated with the similar phagocytic and antigen-presenting functions to the macrophages and mast cells (Mackintosh, 2001; Zhang et al., 2012; Levesque et al., 2013; Richmond et al., 2013; Lin et al., 2018). Additionally, melanocytes could be stimulated by cytokines to coactivate T cells by expressing specific membrane molecules such as intercellular adhesion molecule 1, vascular cell adhesion molecule-1, CD40, and human leukocyte antigen classes I and II (Lu et al., 2002; Christensen et al., 2005; Lin and Fisher, 2007; Zou et al., 2010). Many recent studies have found melanocytes play their immune roles via the TLR signaling pathway

(Cioanca et al., 2018; Morgan et al., 2018; Song et al., 2018). In this work, we found after infected with IBDV, the genes related to dopamine transport, lipid metabolic process, plasma membrane, and integral components of the plasma membrane markedly decreased in the melanocytes. Meanwhile, the genes *CD164, CD226, CD274, CD4*, and *CD7* were highly upregulated suggesting that the melanocytes migration and metabolic pathway were inhibited and increased their abilities to phagocytize and process the viral antigens via specific surface molecule receptors. Our work suggested the melanocytes in the black-boned chicken have important innate immune roles and could modulate other immune cells by up regulating specific cytokines. Moreover, we found lots of melanin were secreted in the nodules of BFs in vivo and widely scattered in the extracellular space of melanocytes in vitro. It has been reported melanin could be transported from the perinuclear area to the cell periphery and dendritic tips along the micro tubular network (McNeil et al., 2004), which protected macrophages from apoptosis by blocking avian influenza virus invasion in vitro (Hu et al., 1999). Therefore, we speculated that abundant melanin secreted from the melanocytes might have protective effects during IBDV invasion and replication.

Previous studies have found that some viruses and bacteria could directly infect human melanocyte and its derived cell lines (Gasque and Jaffar-Bandjee, 2015), which could disturb the melanin synthesis leading to hypopigmentation. We found the IBDV could also induced aberrant melanin synthesis and depigmentation in the BFs, which further supported the hypopigmentation, was highly related to some specific pathogen infection and reminded us the black-boned chicken might be used as an animal model to help us investigate the pathogenic mechanism of aberrant pigmentation in some diseases. In conclusion, our work indicated that the widely distributed melanocytes in the black-boned chicken breeds were kind of immune cells that played important innate immune roles during virus infection. Clarification of melanocyte biology could help us to better understand its atypical migration effect on the chicken development in black-boned chicken, and give some glue to investigate the mechanism of aberrant pigmentation such as albinism, vitiligo, and melanoma.

## ACKNOWLEDGMENTS

This work was supported in part by Chinese University Scientific Fund 2018QC205. National Natural Science Foundation of China: 31872316. Animal Husbandry Science and Technology and Improved Breeding Promotion Capacity Construction Project of Jinan Innovation Zone: 20201028.

## DISCLOSURES

We declare no competing financial interests.

## SUPPLEMENTARY MATERIALS

Supplementary material associated with this article can be found in the online version at doi:10.1016/j.psj.2021.101498.

## REFERENCES

Anello, M., M. S. Daverio, M. B. Silbestro, L. Vidal-Rioja, and F. Di Rocco. 2019. Characterization and expression analysis of KIT and MITF-M genes in llamas and their relation to white coat color. Anim. Genet. 50:143–149.

Byrne, E. H., and D. E. Fisher. 2017. Immune and molecular correlates in melanoma treated with immune checkpoint blockade. Cancer 123:2143–2153.

Chang, C. H., C. J. Kuo, T. Ito, Y. Y. Su, S. T. Jiang, M. H. Chiu, Y. H. Lin, A. Nist, M. Mernberger, T. Stiewe, S. Ito, K. Wakamatsu, Y. A. Hsueh, S. Y. Shieh, I. Snir-Alkalay, and Y. Ben-Neriah. 2017. CK1 alpha ablation in keratinocytes induces p53-dependent, sunburn-protective skin hyperpigmentation. Proc. Natl. Acad. Sci. U S A. 114:E8035–E8044.

Christensen, B. M., J. Li, C. C. Chen, and A. J. Nappi. 2005. Melanization immune responses in mosquito vectors. Trends. Parasitol. 21:192–199.

Cioanca, A. V., P. J. McCluskey, S. S. Eamegdool, and M. C. Madigan. 2018. Human choroidal melanocytes express functional Toll-like receptors (TLRs). Exp. Eye. Res. 173:73–84.

Domyan, E. T., J. Hardy, T. Wright, C. Frazer, J. Daniels, J. Kirkpatrick, J. Kirkpatrick, K. Wakamatsu, and J. T. Hill. 2019. SOX10 regulates multiple genes to direct eumelanin versus pheomelanin production in domestic rock pigeon. Pigment. Cell. Melanoma. Res. 32:634–642.

Dorshorst, B., A. M. Molin, C. J. Rubin, A. M. Johansson, L. Stromstedt, M. H. Pham, C. F. Chen, F. Hallbook, C. Ashwell, and L. Andersson. 2011. A complex genomic rearrangement involving the endothelin 3 locus causes dermal hyperpigmentation in the chicken. PLoS Genet. 7:e1002412.

Dorshorst, B., R. Okimoto, and C. Ashwell. 2010. Genomic regions associated with dermal hyperpigmentation, polydactyly and other morphological traits in the Silkie chicken. J. Hered. 101:339–350.

Faraco, C. D., S. A. Vaz, M. V. Pastor, and C. A. Erickson. 2001. Hyperpigmentation in the Silkie fowl correlates with abnormal migration of fate-restricted melanoblasts and loss of environmental barrier molecules. Dev. Dyn. 220:212–225.

Gasque, P., and M. C. Jaffar-Bandjee. 2015. The immunology and inflammatory responses of human melanocytes in infectious diseases. J. Infect. 71:413–421.

Han, D., S. Wang, Y. Hu, Y. Zhang, X. Dong, Z. Yang, J. Wang, J. Li, and X. Deng. 2015. Hyperpigmentation results in aberrant immune development in Silky Fowl (Gallus gallus domesticus Brisson). PLoS One 10:e0125686.

Han, D., Y. Zhang, J. Chen, G. Hua, J. Li, X. Deng, and X. Deng. 2017. Transcriptome analyses of differential gene expression in the bursa of Fabricius between Silky Fowl and White Leghorn. Sci. Rep. 7:45959.

Han, D. P., S. X. Wang, Y. Y. Zhang, Z. Yang, J. Y. Li, and X. M Deng. 2015. Culture and identification of primary melanocytes from Silky Fowl in vitro. Acta Veterinaria et Zootechnica Sinica 46:949–956.

Henkel, J., C. Lafayette, S. A. Brooks, K. Martin, L. Patterson-Rosa, D. Cook, V. Jagannathan, and T. Leeb. 2019. Whole-genome sequencing reveals a large deletion in the MITF gene in horses with white spotted coat colour and increased risk of deafness. Anim. Genet. 50:172–174.

Hofstetter, S., F. Seefried, I. M. Hafliger, V. Jagannathan, T. Leeb, and C. Drogemuller. 2019. A non-coding regulatory variant in the 5′-region of the MITF gene is associated with white-spotted coat in Brown Swiss cattle. Anim. Genet. 50:27–32.

Hu, G. B., C. Y. Zheng, S. P. Qu, and Y. B. Wei. 1999. Studies on inhibitory effect of melanin on the apoptosis induced by influenza virus in host cells. Virologica Sinica 2:140–146.

Kim, D., G. Pertea, C. Trapnell, H. Pimentel, R. Kelley, and S. L. Salzberg. 2013. TopHat2: accurate alignment of

transcriptomes in the presence of insertions, deletions and gene fusions. Genome. Biol. 14:R36.
Levesque, M., Y. Feng, R. A. Jones, and P. Martin. 2013. Inflammation drives wound hyperpigmentation in zebrafish by recruiting pigment cells to sites of tissue damage. Dis. Mod. Mech. 6:508–515.
Lin, J., X. Yi, and Y. Zhuang. 2020. Coupling metabolomics analysis and DOE optimization strategy towards enhanced IBDV production by chicken embryo fibroblast DF-1 cells. J. Biotechnol. 307:114–124.
Lin, J. Y., and D. E. Fisher. 2007. Melanocyte biology and skin pigmentation. Nature 445:843–850.
Lin, W., F. Su, R. Gautam, N. Wang, Y. Zhang, and X. Wang. 2018. Raf kinase inhibitor protein negatively regulates FcepsilonRI-mediated mast cell activation and allergic response. Proc. Natl. Acad. Sci. U S A 115:E9859–E9868.
Lu, Y., W. Y. Zhu, C. Tan, G. H. Yu, and J. X. Gu. 2002. Melanocytes are potential immunocompetent cells: evidence from recognition of immunological characteristics of cultured human melanocytes. Pigment. Cell. Res. 15:454–460.
Ma, H., S. Zhao, Y. Ma, X. Guo, D. Han, Y. Jia, W. Zhang, and K. Teng. 2013. Susceptibility of chicken Kupffer cells to Chinese virulent infectious bursal disease virus. Vet. Microbiol. 164:270–280.
Mackintosh, J. A. 2001. The antimicrobial properties of melanocytes, melanosomes and melanin and the evolution of black skin. J. Theor. Biol. 211:101–113.
McNeil, E. L., D. Tacelosky, P. Basciano, B. Biallas, R. Williams, P. Damiani, S. Deacon, C. Fox, B. Stewart, N. Petruzzi, C. Osborn, K. Klinger, J. R. Sellers, and C. K. Smith. 2004. Actin-dependent motility of melanosomes from fish retinal pigment epithelial (RPE) cells investigated using in vitro motility assays. Cell Motil. Cytoskeleton 58:71–82.
Morgan, M. D., E. Pairo-Castineira, K. Rawlik, O. Canela-Xandri, J. Rees, D. Sims, A. Tenesa, and I. J. Jackson. 2018. Genome-wide study of hair colour in UK Biobank explains most of the SNP heritability. Nat. Commun. 9:5271.
Muller, H., M. R. Islam, and R. Raue. 2003. Research on infectious bursal disease–the past, the present and the future. Vet. Microbiol. 97:153–165.
Natale, C. A., J. Li, J. Zhang, A. Dahal, T. Dentchev, B. Z. Stanger, and T. W. Ridky. 2018. Activation of G protein-coupled estrogen receptor signaling inhibits melanoma and improves response to immune checkpoint blockade. Elife 7:e31770.
Ortolani-Machado, C., P. De Freitas, M. E. Borges, and C. Faraco. 2008. Special features of dermal melanocytes in white silky chicken embryos. Anat. Rec. 291:55–64.
Richmond, J. M., M. L. Frisoli, and J. E. Harris. 2013. Innate immune mechanisms in vitiligo: danger from within. Curr. Opin. Immunol. 25:676–682.
Shinomiya, A., Y. Kayashima, K. Kinoshita, M. Mizutani, T. Namikawa, Y. Matsuda, and T. Akiyama. 2012. Gene duplication of endothelin 3 is closely correlated with the hyperpigmentation of the internal organs (Fibromelanosis) in silky chickens. Genetics 190:627–638.
Song, H. J., S. H. Lee, G. S. Choi, and J. Shin. 2018. Repeated ultraviolet irradiation induces the expression of toll-like receptor 4, IL-6, and IL-10 in neonatal human melanocytes. Photodermatol. Photoimmunol. Photomed. 34:145–151.
Yu, Y., L. Cheng, L. Li, Y. Zhang, Q. Wang, C. Ou, Z. Xu, Y. Wang, and J. Ma. 2019. Effects of IBDV infection on expression of chTLRs in chicken bursa. Microb. Pathog. 135:103632.
Zekarias, B., W. J. Landman, P. C. Tooten, and E. Gruys. 2000. Leukocyte responses in two breeds of layer chicken that differ in susceptibility to induced amyloid arthropathy. Vet. Immunol. Immunopathol. 77:55–69.
Zhang, W., M. Dai, A. Fridberger, A. Hassan, J. Degagne, L. Neng, F. Zhang, W. He, T. Ren, D. Trune, M. Auer, and X. Shi. 2012. Perivascular-resident macrophage-like melanocytes in the inner ear are essential for the integrity of the intrastrial fluid-blood barrier. Proc. Natl. Acad. Sci. U S A. 109:10388–10393.
Zhao, S., Y. Jia, D. Han, H. Ma, S. Z. Shah, Y. Ma, and K. Teng. 2016. Influence of the structural development of bursa on the susceptibility of chickens to infectious bursal disease virus. Poult. Sci. 95:2786–2794.
Zou, Z., S. W. Shin, K. S. Alvarez, V. Kokoza, and A. S. Raikhel. 2010. Distinct melanization pathways in the mosquito Aedes aegypti. Immunity 32:41–53.